

Contents lists available at ScienceDirect

Biochimica et Biophysica Acta

journal homepage: www.elsevier.com/locate/bbabbio

Q4 Carotenoids are essential for the assembly of cyanobacterial photosynthetic complexes

Q5 Tünde N. Tóth^{a,b,*}, Volha Chukhutsina^b, Ildikó Domonkos^a, Jana Knoppová^{c,d}, Josef Komenda^{c,d}, Mihály Kis^a, Zsófia Lénárt^a, Győző Garab^a, László Kovács^a, Zoltán Gombos^a, Herbert van Amerongen^{b,e}

^a Institute of Plant Biology, Biological Research Centre, Hungarian Academy of Sciences, P.O. Box 521, H-6701 Szeged, Hungary

^b Laboratory of Biophysics, Wageningen University, P.O. Box 8128, 6700 ET Wageningen, The Netherlands

^c Laboratory of Photosynthesis, Institute of Microbiology, Academy of Sciences, Opatovický mlyn, 37981 Trebon, Czech Republic

^d Faculty of Science, University of South Bohemia, Branisovska 31, 37005 Ceske Budejovice, Czech Republic

^e MicroSpectroscopy Centre, Wageningen University, P.O. Box 8128, 6700 ET Wageningen, The Netherlands

1 0 A R T I C L E I N F O

11 Article history:
12 Received 27 April 2015
13 Received in revised form 26 May 2015
14 Accepted 29 May 2015
15 Available online xxx

16 Keywords:
17 Carotenoid deficiency
18 Cyanobacterial photosynthesis
19 Phycobilisome
20 Photosynthetic complexes
21 Time-resolved fluorescence

A B S T R A C T

In photosynthetic organisms, carotenoids (carotenes or xanthophylls) are important for light harvesting, photoprotection and structural stability of a variety of pigment–protein complexes. Here, we investigated the consequences of altered carotenoid composition for the functional organization of photosynthetic complexes in wild-type and various mutant strains of the cyanobacterium *Synechocystis* sp. PCC 6803. Although it is generally accepted that xanthophylls do not play a role in cyanobacterial photosynthesis in low-light conditions, we have found that the absence of xanthophylls leads to reduced oligomerization of photosystems I and II. This is remarkable because these complexes do not bind xanthophylls. Oligomerization is even more disturbed in *crhH* mutant cells, which show limited carotenoid synthesis; in these cells also the phycobilisomes are distorted despite the fact that these extramembranous light-harvesting complexes do not contain carotenoids. The number of phycocyanin rods connected to the phycobilisome core is strongly reduced leading to high amounts of unattached phycocyanin units. In the absence of carotenoids the overall organization of the thylakoid membranes is disturbed: Photosystem II is not formed, photosystem I hardly oligomerizes and the assembly of phycobilisomes remains incomplete. These data underline the importance of carotenoids in the structural and functional organization of the cyanobacterial photosynthetic machinery.

© 2015 Published by Elsevier B.V.

36

38

39

41

1. Introduction

In all living systems carotenoids (Cars) are the most widespread pigments with important structural and functional roles [1]. They can be classified as carotenes and their oxygenated derivatives, the xanthophylls. These pigments can be essential for the assembly of protein complexes [2,3], and for maintaining the membrane integrity [4], but

they might also contribute to the regulation of membrane fluidity [5]. In photosynthetic organisms Cars can function as accessory light-harvesting pigments [6,7], but they also serve as photoprotective agents, especially when the organisms are exposed to excess light [8,9]. In particular, Cars are able to quench triplet excited states of chlorophylls (Chls), and directly scavenge singlet oxygen. Due to their hydrophobic characteristics Cars are mostly localized in the thylakoid membrane, most often in the vicinity of or incorporated in pigment–protein complexes.

Cyanobacteria are prokaryotic photosynthetic organisms, the ancestors of plant chloroplasts. They were fundamental participants in the formation of the oxygenic atmosphere on Earth. Nowadays cyanobacteria represent an ecologically important group especially in the oceans; they have a major role in carbon- and nitrogen-fixation and are often present as symbiotic partners. In cyanobacteria the most abundant Cars are β -carotene and various xanthophylls, such as synechoxanthin, canthaxanthin, caloxanthin, echinenone, myxoxanthophyll, nostoxanthin and zeaxanthin [10,11]. X-ray crystallographic studies have revealed that in the cyanobacterium *Thermosynechococcus elongatus* 22 and 12 β -carotene molecules are located in photosystem I (PSI) [12] and photosystem II (PSII) [13] [7

Abbreviations: APC, allophycocyanin; Car, carotenoid; DAS, decay associated spectrum/spectra; EET, excitation energy transfer; FLIM, Fluorescence Lifetime Imaging Microscopy; LAHG, light activated heterotrophic growth; L_R^{33} , 33 kDa rod linker protein; PAG, photoautotrophic growth; PC, phycocyanin; PBS, phycobilisome; PSI and PSII, photosystems I and II; RC, reaction center; RC47, PSII monomeric core complex lacking CP43; τ_{av} , average lifetime; PPF, Photosynthetic Photon Flux Density; TEs, terminal emitters of the phycobilisomes.

* Corresponding author at: Institute of Plant Biology, Biological Research Centre, Hungarian Academy of Sciences, P.O. Box 521, H-6701 Szeged, Hungary.

E-mail addresses: toth.tunde@brc.mta.hu (T.N. Tóth), chukhutsina@gmail.com (V. Chukhutsina), domonkos.ildiko@brc.mta.hu (I. Domonkos), knoppova@alga.cz (J. Knoppová), komenda@alga.cz (J. Komenda), kis.mihaly@brc.mta.hu (M. Kis), zsolia.lenart@gmail.com (Z. Lénárt), garab.gyozo@brc.mta.hu (G. Garab), kovacs.laszlo@brc.mta.hu (L. Kovács), gombos.zoltan@brc.mta.hu (Z. Gombos), herbert.vanamerongen@wur.nl (H. van Amerongen).

<http://dx.doi.org/10.1016/j.bbabbio.2015.05.020>

0005-2728/© 2015 Published by Elsevier B.V.

Please cite this article as: T.N. Tóth, et al., Carotenoids are essential for the assembly of cyanobacterial photosynthetic complexes, Biochim. Biophys. Acta (2015), <http://dx.doi.org/10.1016/j.bbabbio.2015.05.020>

monomers, respectively. Also the electron transport component, cytochrome *b₆f* (*cyt_{b6}f*) complex, contains a β -carotene molecule [14]. Recently a new, less abundant β -carotene–protein complex, Ycf39–Hlip, was observed in cyanobacteria, which is involved in the early steps of PSII assembly [15]. In the most often used model organism, *Synechocystis* sp. PCC 6803 (hereafter *Synechocystis*), the most common xanthophylls are zeaxanthin, myxoxanthophyll (myxol-2'-fucosid), echinenone, hydroxy-echinenone and synechoxanthin. Hydroxy-echinenone or echinenone serves as an activator switch in the orange carotenoid protein (OCP), which is responsible for non-photochemical quenching in cyanobacteria [16,17] and protects the cells from oxygen radicals [18]. Occasionally, zeaxanthin can also be inserted into OCP, but with lower affinity and eventually this leads to lower efficiency of OCP [19]. The hydrophobic character of carotenoids leads to their preferential presence in the lipid membrane environment. The majority of Cars, especially xanthophylls are located in the outer, cytoplasmic and thylakoid membranes. Most of them are bound to proteins but they can also be constituents of the lipid phase [10], where they can influence the membrane dynamics and microviscosity [5] and perform protective roles [5,20]. Although the amounts of the xanthophyll molecules and their distribution among the cell compartments are influenced by environmental conditions [21,22], they can be predominantly found in the thylakoid membranes. It is generally accepted that in cyanobacteria zeaxanthin and myxoxanthophyll provide efficient protection against photooxidation and lipid peroxidation under various stress conditions [20,22,23]. In addition, myxoxanthophyll appears to be an important factor in maintaining extended thylakoid membrane sheets [4]. Less information is available about the role of synechoxanthin [24], but it seems that it is mostly present in the

cell membrane, and participates in protecting the cells against high light exposure [25].

Biosynthesis of carotenoids in cyanobacteria has been intensively studied and several mutants deficient in different Cars are available [10,11]. In the $\Delta crtRO$ double mutant strain of *Synechocystis* an almost complete loss of xanthophylls was obtained by the inactivation of two biosynthetic enzymes (carotene β -ketolase and carotene β -hydroxylase) [26] and thus the mutants contain only β -carotene, synechoxanthin and a myxoxanthophyll precursor, namely deoxy-myxol-2'-dimethyl-fucosid (Fig. 1). The basic photosynthetic processes and membrane integrity appear to be unaffected in this mutant; only the light sensitivity of the cells in high-light intensities increases [26,27]. The *crtH* mutant strain is deficient in the CrH enzyme, which catalyzes the *cis*-to-*trans* isomerization of carotenoids at the early steps of their synthesis. Photo-isomerization can still occur if the cells are cultivated under continuous light conditions [28]. However, photo-isomerization is unable to completely replace the enzymatic *cis*-to-*trans* isomerization [28,29]; the light-grown *crtH* and wild-type cells contain the same Car species, but the ratio of the various Cars is somewhat different [28] (Fig. 1), whereas the dark-grown *crtH* cells are unable to synthesize *trans*-carotenoids due to the lack of both enzymatic and photo-isomerization. This strain can produce only some Car precursors, primarily *cis*-lycopenes and a small amount of all-*trans* carotenes, but no xanthophylls [28,29].

Recently, a completely Car-free $\Delta crtH/B$ mutant strain has been generated by the inactivation of the *crtB* gene, encoding the phytoene synthase in *crtH* cells [30]. The $\Delta crtH/B$ mutant cells do not contain phytoene or any downstream carotenoid biosynthesis intermediates. The $\Delta crtH/B$ cells are extremely light sensitive and only capable of growing in the dark, under light-activated heterotrophic growth (LAHG) [27

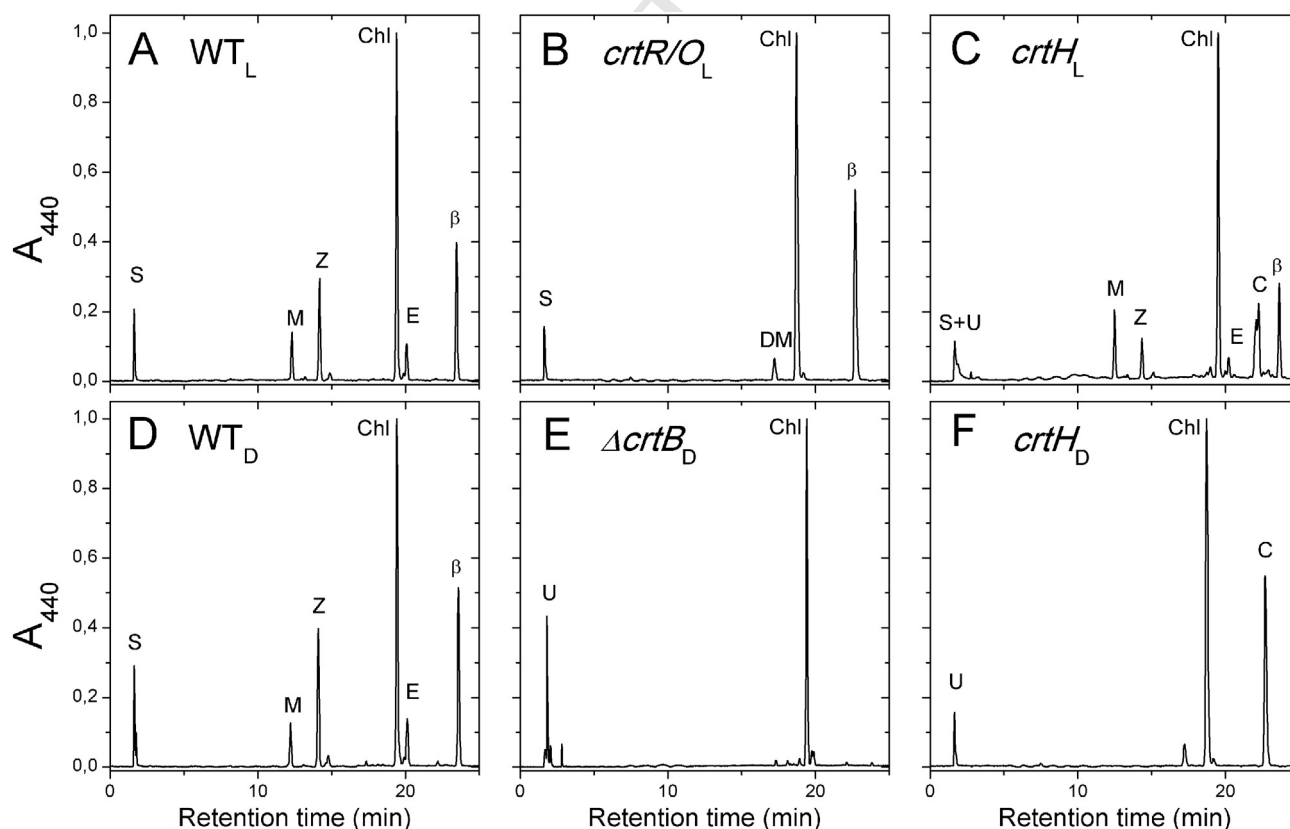


Fig. 1. HPLC analysis of photosynthetic pigment extracts of wild-type and mutant cells. Chromatograms of WT_L (A); *crtR/O_L* (B); *crtH_L* (C); WT_D (D); $\Delta crtB_D$ (E), and *crtH_D* (F) cells were recorded at 440 nm. The samples containing equivalent chlorophyll concentrations were loaded. Car derivatives were identified on the basis of both their absorption spectra and their retention times. β , β -carotene; C, *cis*-carotenes; Chl, chlorophyll; DM, deoxy-myxoxanthophyll; E, echinenone; M, myxoxanthophyll; U, unknown non-carotenoid derivatives; Z, zeaxanthin.

conditions [31], like the Car deficient green algae [3]. Cells of the cyanobacterial $\Delta crtH/B$ mutant possess no oxygen-evolving capacity, suggesting the absence of photochemically active PSII complexes and/or the absence of a functional water-splitting enzyme. In these cells only a small amount of non-functional, partially assembled PSII core complex can be detected [30]. However, *cyt_bf* complexes were present in these cells [30], as in the Car-deficient green algae [3]. The thylakoid structure is also influenced by the mutations as only a few fragmented thylakoids were found in the mutant cells [10]. For the current study, in order to investigate the effect of Car deficiency, we have generated a new $\Delta crtB$ single mutant, which led essentially to the same results as the $\Delta crtH/B$ double mutant.

In summary, in the photosynthetic machinery of cyanobacteria the xanthophylls seem to play a role only under stress conditions, while the additional lack of β -carotene has far more severe effects.

In photosynthetic organisms, the pigment–protein complexes embedded in the thylakoid membrane carry out the conversion of light energy into chemical energy. The various pigments contained in the photosynthetic complexes have distinct characteristics to ensure the optimal funneling of excitation energy toward the photosynthetic reaction centers (RCs) [6]. Both photosystems (PSII and PSI) have highly conserved protein structures. In cyanobacteria and plants PSII core is present in a dimeric multi-protein complex of approx. 20 proteins. Each monomer contains two inner antennae, CP43 and CP47 and the RC, which is composed of the D1 and D2 proteins and the cytochrome *b*₅₅₉. PSII possesses a total of 35 chlorophylls *a* (Chl *a*) per monomer. Despite the high structural homology of PSI in plants and cyanobacteria, in cyanobacteria PSI often exists as a trimer instead of a monomer, which is the dominant form in plants. The PSI core complex consists of PsaA and PsaB proteins and several small molecular weight subunits. It harbors the RC and inner antenna and per PSI monomer 96 Chl *a* are bound. The main differences between cyanobacterial and plant PSI reside in their low molecular weight protein constituents. Some of these small molecular weight proteins were proven to be important for trimerization of the PSI monomers into trimers [12]. The most important of these subunits is the PsaL protein, which is necessary for trimerization, whereas PsaM and PsaI have a trimer-stabilizing function. Chl *a* has an *in vivo* absorption maximum typically at ~680 nm and emits fluorescence at ~685 nm except for a few long-wavelength Chl *a* molecules (LWCs) in PSI, emitting at longer (~730 nm) wavelengths. The LWC molecules are more abundant in PSI trimers than in monomers due to some pigment–pigment interactions, which are only present in the trimer [12]. Although the exact position and role of LWCs are controversial, the emitted long-wavelength fluorescence is often used as an *in vivo* sign of the presence of PSI trimers [32].

In cyanobacteria, peripheral antenna complexes, the phycobilisomes (PBSs), serve as light-harvesting antennae for the photosynthetic complexes [33]. In PBSs the phycobilin pigments (phycocyanobilin, phycoerythrobilin, phycobiliviolin) attached to phycobiliproteins (phycocyanin, allophycocyanin, phycoerythrin, phycoerythrocyanin) are responsible for light harvesting. In *Synechocystis* each PBS contains approximately six phycocyanin (PC) rods attached to the three allophycocyanin (APC) core cylinders. Each PC rod comprises typically three hexameric disks (18 bilins/hexamer) while all the APC core cylinders consist of four trimeric disks (6 bilins/trimer). There are various linker proteins, which are responsible for maintaining the PBS structure, and these linkers can be divided into groups according to their function [34]. The rod linker (*L_R*) proteins attach to the hexameric rod units and organize them into rods [35]. The different *L_R* proteins are named according to their molecular masses. The *L_R*¹⁰ protein is believed to be localized at the end of the rods as a cap and has a stabilizing function. *L_R*³⁰ attaches the last hexameric unit to the middle one, while *L_R*³³ is required for the linkage of the first and second units. The rod-core linkers (*L_{RC}*) bind the rods to the core cylinders. The small core linkers (*L_C*) stabilize the core cylinders and the membrane-core linker (*L_{MC}*) anchors the PBSs to the PSs [34].

The incident light is absorbed mainly by the pigments of the PC rods, which have maximum absorbance at around 620 nm and fluorescence emission maximum at 640–650 nm. As a next step, the absorbed energy is transferred to the pigments of the APC in the PBS core with 650 nm absorption. The two core cylinders closest to the membrane contain some special APC trimers [36], that function as terminal emitters (TEs) of the PBSs. These special trimers possess low-energy bilins, which ensure the direct excitation energy transfer (EET) to the Chl *a*-containing photosystem cores [37]. Most of the APC trimers show fluorescence emission around 660 nm (APC₆₆₀), while the TEs fluoresce at around 680 nm (APC₆₈₀).

The fluorescence emitted by the pigment–protein complexes can provide information about the rate and efficiency of various photosynthetic processes. Although a wealth of information is available about the function of Cars in cyanobacteria, no systematic comparative study has been performed in these organisms on their specific role on the excitation energy transfer processes in the light-harvesting antenna, and in the assembly and stability of the main constituents of the thylakoid membranes.

The present study focuses on the role of various Cars in the functional organization of the photosynthetic complexes in *Synechocystis* cells. We studied several *Synechocystis* mutants impaired at various Car biosynthetic steps and characterized them using picosecond fluorescence spectroscopy or microscopy combined with biochemical methods and electron microscopy. Our results show that the various Car classes influence the membrane organization, assembly and oligomerization of PSI and PSII to different extents. Furthermore, we have found that the structure of PBS strongly depends on the Car composition of the thylakoid membranes, despite the fact that carotenoids are known not to be present in PBSs.

2. Methods

2.1. Cell culturing

Synechocystis sp. PCC 6803 cells were cultivated in BG11 medium [38] buffered with 5 mM HEPES (pH 7.5) on a rotary shaker at 30 °C. The cells were grown either under photoautotrophic growth (PAG) conditions for WT, *crtR/O* and *crtH* [28] (WT_L, *crtR/O_L* and *crtH_L*) or under light-activated heterotrophic growth (LAHG) conditions [31] for the $\Delta crtB$, *crtH* and WT strains ($\Delta crtB_D$, *crtH_D* and WT_D). Under PAG conditions the cells were illuminated with continuous white light using 35 $\mu\text{mol photons m}^{-2} \text{s}^{-1}$ PPFD (Photosynthetic Photon Flux Density). Under LAHG conditions BG11 was supplemented with 10 mM glucose and daily pulses of 20 $\mu\text{mol photons m}^{-2} \text{s}^{-1}$ PPFD light was provided for 10 min per day. The mutant cells were cultured in the presence of the appropriate antibiotics (40 $\mu\text{g ml}^{-1}$ spectinomycin for *crtR/O* and $\Delta crtB$, 40 $\mu\text{g ml}^{-1}$ kanamycin for *crtR/O* and *crtH*). The cells were harvested during the logarithmic growth phase.

2.2. Construction of *Synechocystis* sp. PCC 6803 $\Delta crtB$ and *crtR/O* mutant strains

A construct containing part of the *crtB* gene and an omega cassette [30] were used to transform WT cells of *Synechocystis* sp. PCC 6803. Transformants were selected under LAHG conditions on BG11 agar plates supplemented with glucose and increasing concentration of spectinomycin by several restreakings of single colonies.

The *crtR/O* mutant was a gift from Kazumori Masamoto (Kumamoto University, Japan). This mutant was created by introducing kanamycin and spectinomycin cassettes into the coding regions of the *crtR* and *crtO* genes, respectively. Complete segregation of the mutant cells was confirmed by PCR.

2.3. Pigment analysis

The cells were harvested by centrifugation, frozen in liquid nitrogen and stored at $-80\text{ }^{\circ}\text{C}$ until the extraction. Pigments were extracted with 100% methanol and passed through a PTFE 0.2- μm pore size syringe filter. Samples containing equivalent amounts of chlorophyll were separated by high-pressure liquid chromatography (HPLC) on a Shimadzu LC-20 HPLC system using a $4.6 \times 250\text{-mm}$ ReproSil-Pur Basic RP-18 column with 5 μm particle size (Dr. Maisch, Ammerbuch, Germany). The columns were equilibrated with solvent of acetonitrile:water:triethylamine (9:1:0.01) and eluted with one step linear gradient (25 min) of 100% ethylacetate at a constant flow rate of 1 ml min^{-1} . Car derivatives were identified on the basis of both their absorption spectra and their retention times. The relative content of pigments was estimated by a comparison of peak areas on chromatograms recorded at 440 nm. The concentrations of carotenoid species were calculated from Beer–Lambert’s law using their specific extinction coefficients at 440 nm [39]. The values are the means \pm SD of at least three independent experiments.

2.4. Electron-microscopy analysis

The collected cells were fixed in 1% paraformaldehyde and 1% glutaraldehyde for 4 h at $4\text{ }^{\circ}\text{C}$ and post-fixed in 1% osmium tetroxide. The samples were dehydrated and further treated according to the standard procedure described earlier [40].

2.5. Isolation of phycobilisomes

Phycobilisomes were prepared from *Synechocystis* sp. PCC 6803 wild-type and mutant cells according to [41] with some modifications. Cells were pre-treated with 0.2% lysozyme at $37\text{ }^{\circ}\text{C}$. The cells were disrupted with 0.1 mm diameter glass beads in 0.75 M K–Na phosphate buffer (pH 7.0) using a Bead Beater homogenizer. After 5% Triton X-100 treatment for 50 min at room temperature the thylakoid membranes were pelleted by centrifugation at 15,000 g. The supernatant was treated again with 3% Triton X-100 for 20 min prior to loading onto a discontinuous sucrose density gradient. After 20 h of centrifugation at 90,000 g at $14\text{ }^{\circ}\text{C}$ the PBS containing blue-colored layers were removed from the gradients and stored at room temperature until spectroscopic and protein analysis was applied.

2.6. Protein analysis

Membranes for two-dimensional blue native/denaturing polyacrylamide gel electrophoresis (BN/SDS–PAGE) were isolated by breaking cells in 25 mM MES/NaOH buffer (pH 6.5) containing 10 mM CaCl_2 , 10 mM MgCl_2 and 25% glycerol using glass beads in a beadbeater. The thylakoid membranes were collected by centrifugation and were solubilized with 1% dodecyl- β -D-maltoside. First-dimension, blue-native electrophoresis was performed at $4\text{ }^{\circ}\text{C}$ in a 4–14% polyacrylamide gel. 5 μg Chl containing samples were loaded onto each lane. The protein composition of the complexes was assessed by second-dimension electrophoresis in a denaturing 12 to 20% linear gradient polyacrylamide gel containing 7 M urea. The lanes from the native gel were excised along their entire length, incubated for 20 min in 25 mM Tris/HCl (pH 7.5) containing 1% SDS and 1% dithiothreitol (w/v) and placed on top of the denaturing (SDS) gel. Proteins separated in the gel were stained with Coomassie Blue [42]. Identification of the protein bands was performed either by specific antibodies or by MS as described in Knoppova et al. [15].

Protein composition of isolated PBSs was studied using Tricine–SDS–PAGE 10 to 16% linear gradient according to Schagger [43]. The isolated PBSs were precipitated by adding an equal volume of 20% trichloroacetic acid and incubating on ice for 5 min. After centrifugation the pellet

was resuspended in loading buffer and heated for 5 min at $85\text{ }^{\circ}\text{C}$. 40 μg of total protein containing samples was loaded onto each lane. The separated proteins were stained with Coomassie Blue.

2.7. Picosecond time-resolved measurements

Two-photon excitation (860 nm) Fluorescence Lifetime Imaging Microscopy (FLIM) measurements were performed as described in [44]. Fluorescence was detected through a band-pass (BP) filter of 647 nm with 58 nm bandwidth (BP 647/58) with time steps of 12 ps per channel. 64×64 pixel images were collected with $0.2\text{ }\mu\text{m} \times 0.2\text{ }\mu\text{m}$ pixel resolution. Low excitation power (60 μW average power at 860 nm) was used in combination with long integration times (20–30 min). Cells were immobilized in 3% low gelling temperature agarose, type VII (Sigma-Aldrich), dissolved in BG11 media. FLIM images were analyzed using Glotaran as graphical user interface for the R-package TIMP (glotaran.org) [45]. Only pixels with fluorescence intensity above 75 counts per second were selected for global analysis. Global analysis of the image results in the same set of lifetimes for all selected pixels whereas the amplitudes can vary. The amplitude-weighted average lifetimes were calculated as described in [44,46].

Time-resolved emission spectra were recorded at room temperature (293 K) with a synchroscan streak-camera system [47] using 100–200 fs laser excitation pulses centered around 590 or 400 nm. The time window was either 800 ps or 2 ns. The laser repetition rate was 250 kHz and the laser power was typically 70 μW with a spot size of $\sim 100\text{ }\mu\text{m}$ (diameter). Cells with an optical density of 0.3–0.6 cm^{-1} at the excitation wavelength were used for the measurements. The cells were dark-adapted for 10 min before and circulated in a 1 mm flow cell during the measurements with a flow speed of $\sim 2.5\text{ ml/s}$.

Images were corrected for the background and photocathode shading, and then sliced up into traces of 5 nm width. Global analysis of the streak images was performed using the Glotaran graphical user interface for TIMP [48]. Data obtained with 800 ps and 2 ns time windows were linked during the global analysis. A single, Gaussian-shaped instrument response function was used for the analyses and its width was a free fitting parameter resulting in typical value between 4–6 ps for the 800 ps and 10–12 ps for the 2 ns time window, respectively.

3. Results

3.1. Carotenoid composition of the different strains

The xanthophyll deficient *crtR/O* mutant can grow photoautotrophically (hereafter *crtR/O_L*), while the completely carotenoid-less Δ *crtB* possesses extreme light sensitivity and is only capable of growing in the dark, under light-activated heterotrophic growth conditions (hereafter Δ *crtB_D*). We also studied the *crtH* mutant either cultivated under photoautotrophic or light activated heterotrophic growth conditions (hereafter *crtH_L* and *crtH_D*, respectively). In order to distinguish the carotenoid induced changes from the ones induced by the growth conditions, the wild type cells were grown under photoautotrophic and light activated heterotrophic growth conditions as well (hereafter *WT_L* and *WT_D*, respectively).

The pigment composition of mutants used in this study was determined by HPLC (Fig. 1). The carotenoid composition of the *WT_D* cells does not differ significantly from *WT_L*. The xanthophyll-deficient *crtR/O_L* cells contain no zeaxanthin, echinenone, but have deoxy-myxoxanthophyll instead of the myxoxanthophyll [26]. In the *crtH* mutant a large amount of *cis*-carotene is present under both growth conditions indicating that the isomerization of the *cis*-carotene is the rate-limiting step of the synthesis [28]. A small amount of unknown non-carotenoid derivatives was also observed in *crtH_L* and *crtH_D*. In addition, in *crtH_L* cells all carotenoid classes are present but their relative amounts are different than in the *WT*. The estimated molar ratio of β -carotene to Chl is 0.131 ± 0.003 in

373 WT_L and 0.097 ± 0.008 in *crtH_L*. In *crtH_D* cells grown in the dark no β -
 374 carotenes or xanthophylls are present. The carotenoid deficient
 375 Δ *crtB_D* cells contain only chlorophyll and a small amount of un-
 376 known non-carotenoid derivatives, similar to what was observed
 377 previously for Δ *crtH/B* [30].

378 3.2. Electron microscopy analysis

379 The effect of Cars on thylakoid membrane organization was investi-
 380 gated by standard transmission electron microscopy. The xanthophyll-
 381 deficient *crtR/O_L* and the *crtH_L* cells show similar morphology as WT
 382 *Synechocystis* cells (Fig. 2). All strains contain multi-layered membrane
 383 sheets of 3–6 pairs of thylakoids running mostly parallel to the cytoplas-
 384 mic membrane within the peripheral region of the cell and occasionally
 385 some thylakoid membrane pairs traverse the central cytoplasm. The av-
 386 erage distance between adjacent membrane pairs is approximately
 387 40 nm, which is a typical value for WT *Synechocystis* cells [49].

388 The dark-grown WT_D cells exhibit a reduced number of thylakoid
 389 layers in a less-ordered structure than WT_L cells (Fig. 2). Only short sec-
 390 tions of membrane pairs run parallel to the cell wall with slightly in-
 391 creased inter-thylakoidal distances (~50 nm) and more thylakoid
 392 sheets are penetrating into the central region of the cell. The complete
 393 lack of Cars in the Δ *crtB_D* cells and *crtH_D* cells, however, results in
 394 more disorganized thylakoid structures than in WT_D cells. In both the
 395 Q15 Δ *crtB_D* and *crtH_D* cells, the thylakoids do not form multilayer mem-
 396 branes parallel to the cell wall but only membrane pairs randomly dis-
 397 tributed in the cell. The distance between adjacent thylakoid sheets
 398 increases to 60–140 nm and membrane pairs enclose a slightly inflated
 399 thylakoid lumen. In summary, the absence of xanthophylls or limited
 400 availability of carotenoids leaves the thylakoid structure intact but the
 401 complete absence of carotenoids largely disturbs the ultrastructure of
 402 thylakoid membranes.

403 3.3. Protein analysis of thylakoid membranes

404 We have investigated the presence of thylakoid-membrane proteins
 405 and their complexes by 2D gel electrophoresis (Fig. 3). In the first

406 dimension, native protein complexes, obtained by mild solubilization
 407 of thylakoid membranes, were separated and in the second dimension,
 408 the subunit composition of the complexes was determined by denatur-
 409 ing SDS-PAGE, allowing the detection and quantification of the different
 410 oligomeric forms of PSI, PSII, and other proteins/complexes.

411 In WT_L cells (under PAG conditions) PSII is predominantly present as
 412 a dimeric core complex (arrows 1), closely followed by PSII core mono-
 413 mers, while the amount of RC47 (monomeric PSII core lacking CP43) is
 414 negligible (arrow 2). PSI predominantly exists as trimers (arrows 3 and
 415 4) while the level of PSI monomers is much lower (arrows 7 and 8) and
 416 the amount of PSI dimers is negligible (arrows 5 and 6). Interestingly,
 417 PSI trimers (unlike monomers and dimers) show strong resistance
 418 against SDS-induced disassembly and only the small subunits PsaF
 419 and PsaE are significantly released during SDS-PAGE while the large
 420 PsaA and PsaB subunits remain together with the majority of PsaD
 421 and PsaL.

422 Xanthophyll-deficient *crtR/O_L* cells show a significantly lower level
 423 of PSII dimers and PSI trimers (arrow 1) than WT_L cells (arrows 2 and
 424 3) and a concomitant increase of the monomeric form of these com-
 425 plexes, indicating destabilization of oligomerization in the absence of
 426 xanthophylls. These results confirm the overall stabilization effect of
 427 xanthophylls on the structure of PSI trimers.

428 The *crtH_L* strain contains an even lower amount of PSII dimers as
 429 compared to monomers and the level of RC47 is higher than in WT_L.
 430 Also the PSI trimer to monomer ratio is far lower than in WT_L and PSI tri-
 431 mers are more efficiently disassembled by SDS. Our results show a more
 432 severe effect on photosystem complexes upon β -carotene limitation
 433 than in the absence of xanthophylls only.

434 2D gel electrophoresis was also applied to the WT_D strain (Fig. 3) and
 435 the Δ *crtB_D* and *crtH_D* strains. As compared to WT_L, the amount of dimeric
 436 PSII core complexes is drastically reduced, and the amount of RC47
 437 has increased in the WT_D strain. In both Δ *crtB_D* and *crtH_D* strains, how-
 438 ever, the PSII complexes are almost completely absent and a trace
 439 amount of RC47 is the only PSII complex detectable by protein staining
 440 in both mutants.

441 The strong depletion (*crtH_D*) or absence (Δ *crtB_D*) of Cars also leads to
 442 the almost complete lack of PSI trimers and the presence of mostly

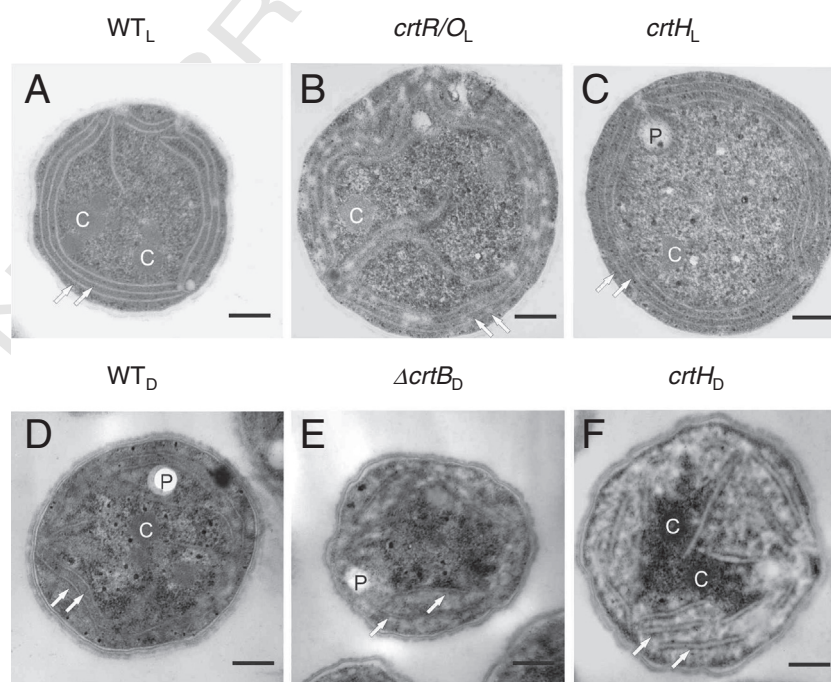


Fig. 2. Electron micrographs of *Synechocystis* sp. PCC 6803 wild-type and carotenoid biosynthesis mutant strains. White arrows indicate thylakoid membrane pairs in WT_L (A); *crtR/O_L* (B); *crtH_L* (C); WT_D (D); Δ *crtB_D* (E), and *crtH_D* (F) cells. C: Carboxysome; P: polyphosphate bodies. Bars: 0.25 μ m.

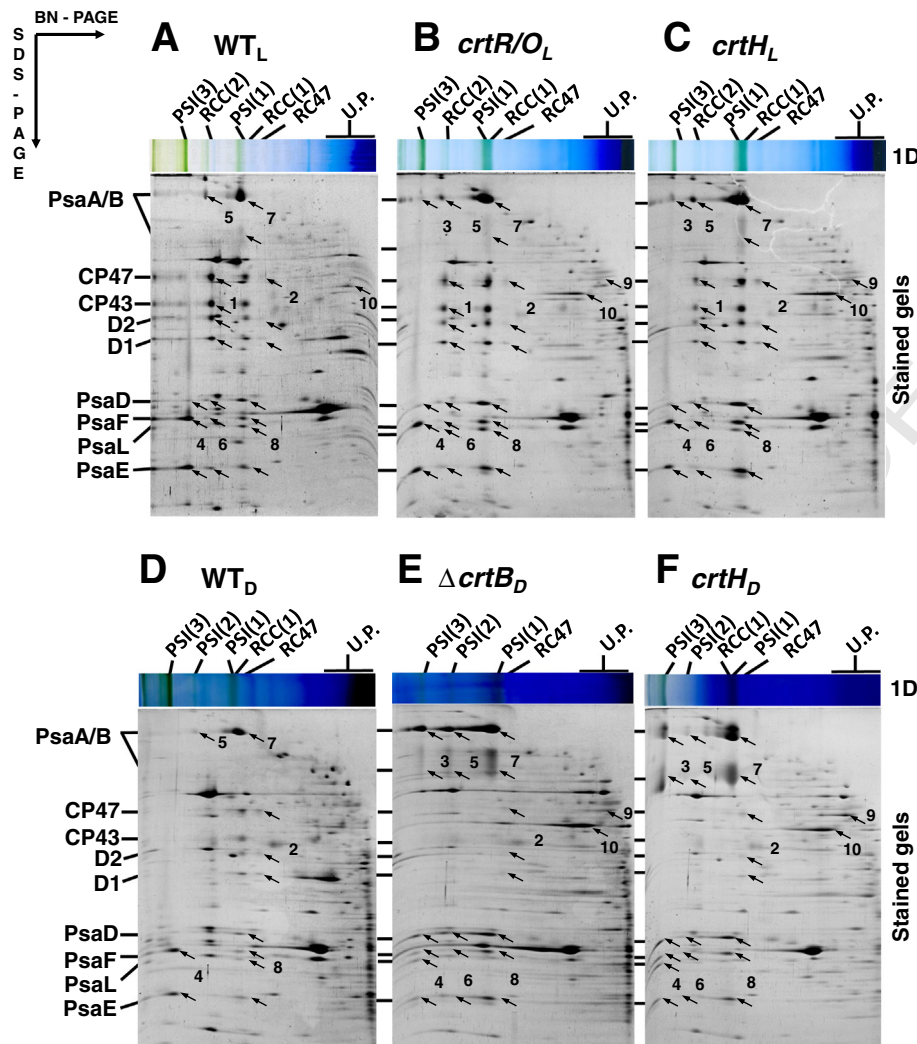


Fig. 3. Two dimensional BN/SDS-PAGE analysis of thylakoid membranes of the various strains. Thylakoids were isolated from WT_L (A); *crtR/O_L* (B); *crtH_L* (C); WT_D (D); Δ *crtB_D* (E), and *crtH_D* (F) cells. Designation of complexes: PSI(3), PSI(2) and PSI(1), trimeric, dimeric and monomeric PSI complexes, respectively; RCC(2) and RCC(1), dimeric and monomeric PSII core complexes, respectively; RC47, PSII core complex lacking CP43; U.P., unassembled proteins. Arrows 1 – large subunits of RCC(2) CP47, CP43, D2 and D1 proteins (from top to bottom), arrows 2 – large subunits of RC47 CP47, D2 and D1 proteins (from top to bottom); arrows 3 – large subunits of PSI(3); arrows 4 – small subunits of PSI(3) PsaD, PsaF, PsaL and PsaE (from top to bottom); arrows 5 – large subunits of PSI(2); arrows 6 – small subunits of PSI(2); arrows 7 – large subunits of PSI(1); arrows 8 – small subunits of PSI(1); arrow 9 – ChlP, geranylgeranyl reductase; arrow 10 – PstS1 phosphate transporter.

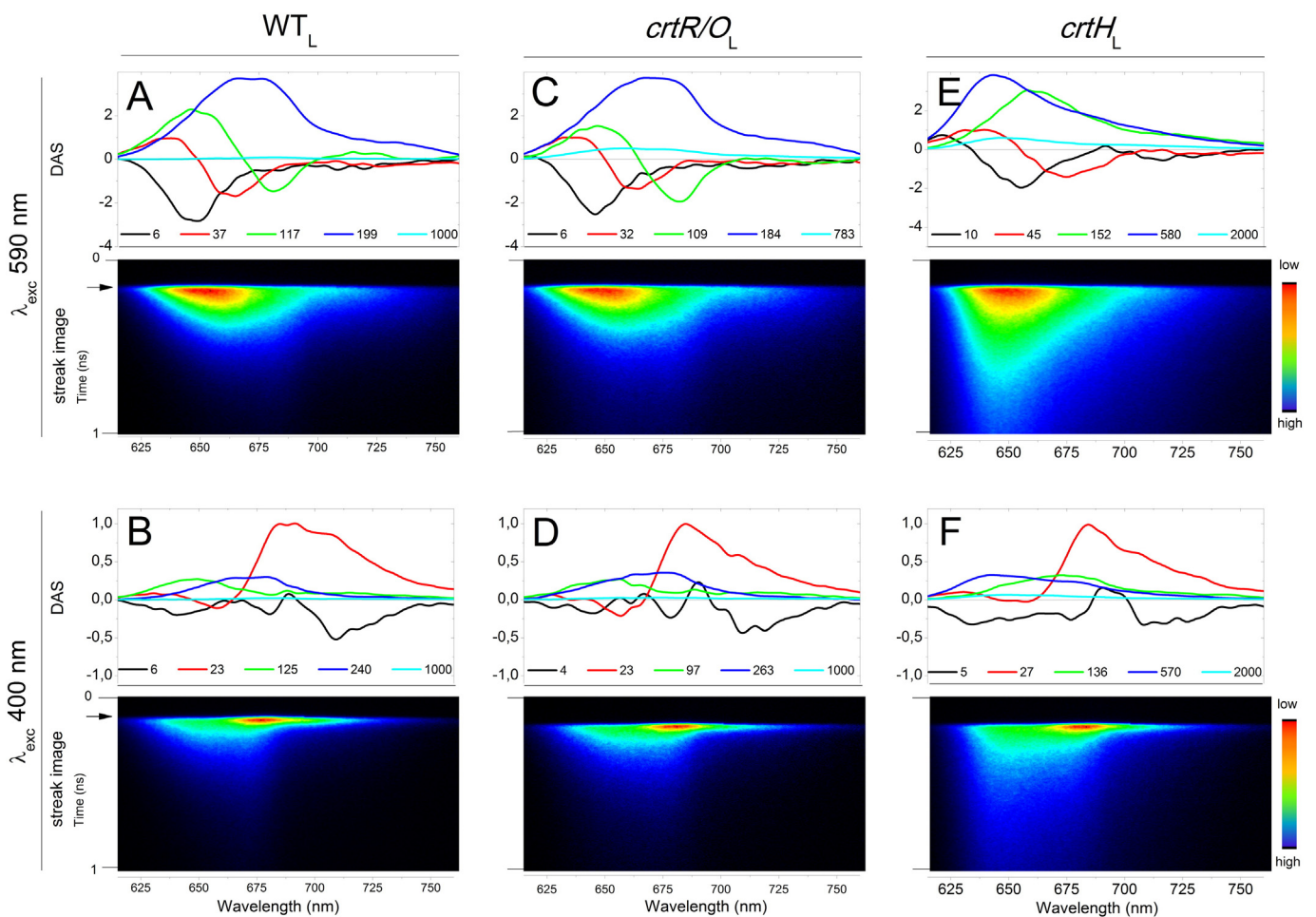
443 monomers or occasionally dimers, in contrast to the dominance of trimers in WT_D cells. Also the stability of the PSI complexes is largely affected as indicated by their decreased stability of the native complex during SDS-PAGE. Interestingly, Δ *crtB_D* PSI monomers are lacking the PsaL subunit while the trimers still contain it. The PsaL subunit is easily released from the trimers of the mutants but not from WT_D and WT_L trimers. This indicates that PsaL binding in the trimer-forming domain of the PSI monomer is destabilized in the absence of Cars, leading to its release from the monomer during BN-PAGE. In summary, PSII complexes are not formed in the absence of carotenoids, whereas PSI complexes are still formed but PSI monomers dominate.

454 3.4. Streak-camera measurements of whole cells

455 The process of excitation energy transfer (EET) can be monitored particularly well with time-resolved fluorescence techniques. Photosynthetic systems have relatively short fluorescence decay times if both EET and charge separation (CS) are efficient. In cyanobacteria light is mainly captured by PBSs and the excitation energy is transferred toward the RCs, where it is used for CS, thereby leading to relatively short fluorescence lifetimes. In the case of open PSII RCs no long,

1–2 ns fluorescence lifetimes are present, unless EET energy is blocked somewhere. Here we studied EET and CS in mutant cells using streak-camera measurements (Fig. 4) and applying two excitation wavelengths: the 590 nm light mainly excites the PBSs (90%) and the 400 nm light excites mainly the Chls but also PBSs to some extent [17].

467 Global analysis of streak-camera data obtained for WT_L cells (Fig. 4) results in similar decay-associated spectra (DAS) as observed and discussed before for cells under similar conditions [17]. Upon 590 nm excitation (Fig. 4A) five components are observed: the 6–8 ps (black color line) DAS reflects excitation equilibration within the PC rods of the PBSs, the 30 ps (red color line) DAS shows downhill EET from PC to APC₆₆₀ with the typical positive sign on the short-wavelength side (corresponding to fluorescence decay) and the negative sign at longer wavelengths (corresponding to a rise of fluorescence due to EET to the corresponding pigments). The 117 ps (green color line) component reflects EET from APC₆₆₀ to APC₆₈₀ + Chls and the 199 ps (blue color line) component is due to excitation trapping by the RCs (charge separation). Also a long-lived component (~1 ns) can be observed (cyan color line), which has very low amplitude and probably reflects competition between secondary charge separation and charge recombination [17,50].



Q1 **Fig. 4.** Streak images and decay-associated spectra of light grown strains. Data obtained for WT_L (A, B), crtR/O_{PAG} (C, D) and crtH_{PAG} (E, F) cells are shown. DAS were obtained from global fitting of the time-resolved fluorescence data recorded with the streak camera. The corresponding lifetimes are given in the figures in ps. The excitation wavelengths were 590 nm and 400 nm, as indicated. The spectra are normalized to the second (red color line) lifetime component. Streak images show 1 ns time windows of the fluorescence kinetics. Arrows represent the start of the fluorescence.

483 Upon 400 nm excitation (Fig. 4B) the fluorescence components originate from different pigment–protein complexes and they are less easily
 484 separated into various processes: the 6 ps DAS component (black color line) reflects both equilibration within PC rods (see above) and EET in
 485 PSI from bulk to red Chls [44]. The dominating 21 ps (red color line) component represents mainly CS in PSI (leading to decay of Chl fluores-
 486 cence) but it also shows some contribution of the ~30 ps PBS component, which is observed upon 590 nm excitation. The 125 ps
 487 component (blue color line) shows characteristics of the 117 ps (down-hill EET) and 199 ps components (charge separation in PSII) observed
 488 upon 590 nm excitation. The 240 ps component is rather similar to the 199 ps DAS in Fig. 3 (panel A) and is most probably due to CS in PSII.
 489
 490 Although the DAS of crtR/O_L cells (Fig. 4C and D) were similar to those of WT cells grown under the same conditions, a fraction of long-
 491 lived (783 ps) fluorescence could be observed (590 nm excitation) with PBS spectral characteristics (max 660 nm), which was not
 492 observed for WT cells. This component reflects a small fraction of distorted PBSs or PBSs that are badly connected to the PSs. 400 nm excitation
 493 leads to similar results as for WT_L cells. Although, a decreased amount of PSII dimers is observed by 2D-PAGE (Fig. 3), the *in vivo* PSII fluores-
 494 cence is not influenced in the mutant significantly. However, the PSI DAS (~23 ps) shows less contribution on the long-wavelength side
 495 (above 700 nm), reflecting less red pigments in PSI.

496 For crtH_L cells the obtained DAS and corresponding lifetimes are different from those of WT_L (Fig. 4C). Upon 590 nm excitation there is no
 497 clear component for EET from the PBSs to the pigments fluorescing around 675–680 nm (Chls and some red-shifted bilins in the core of
 498 the PBSs) [51]. For these cells dominant ~600 ps and less pronounced ~2 ns components are present with a maximum of around
 499 640–650 nm. These components originate mostly from energetically disconnected PC units, showing that PBSs are to a large extent not
 500 assembled. In addition, the ~600 ps component has a shoulder around 680 nm which is more pronounced upon 400 nm excitation demon-
 501 strating that it is partly due to Chl *a*. This long-lived Chl fluorescence might originate from the RC47 complex observed with 2D-PAGE
 502 (Fig. 3) due to the incomplete assembly of PSII. On the other hand, the PSI signal is similar to that obtained for crtR/O_L cells (red color line).
 503 For WT_D cells a smaller fraction of functionally coupled PBS–PSII complexes is detected than for WT_L cells, which is reflected in the smaller
 504 negative amplitude of the green color line DAS and the smaller amplitude of the blue color line DAS upon 590 nm excitation (Fig. 5A).
 505 In addition, a fraction of long-lived, ~1.3 ns fluorescence is observed originating from functionally disconnected PBSs. Upon 400 nm excitation
 506 the PSI signal has a similar shape as observed for WT_L, *i.e.* with the pronounced shoulder above 700 nm.

507 The lack or strong decrease of Cars induces drastic increase (3-fold) in the fluorescence decay time of the *Synechocystis* cells (Δ crtB_D and
 508 crtH_D) when compared to WT_D (see Fig. 5 streak camera images). The obtained DAS are very similar for Δ crtB_D and crtH_D cells. Upon 590 nm
 509 excitation the dominating blue color line DAS with ~700 ps lifetime

510
 511
 512
 513
 514
 515
 516
 517
 518
 519
 520
 521
 522
 523
 524
 525
 526
 527
 528
 529
 530
 531
 532

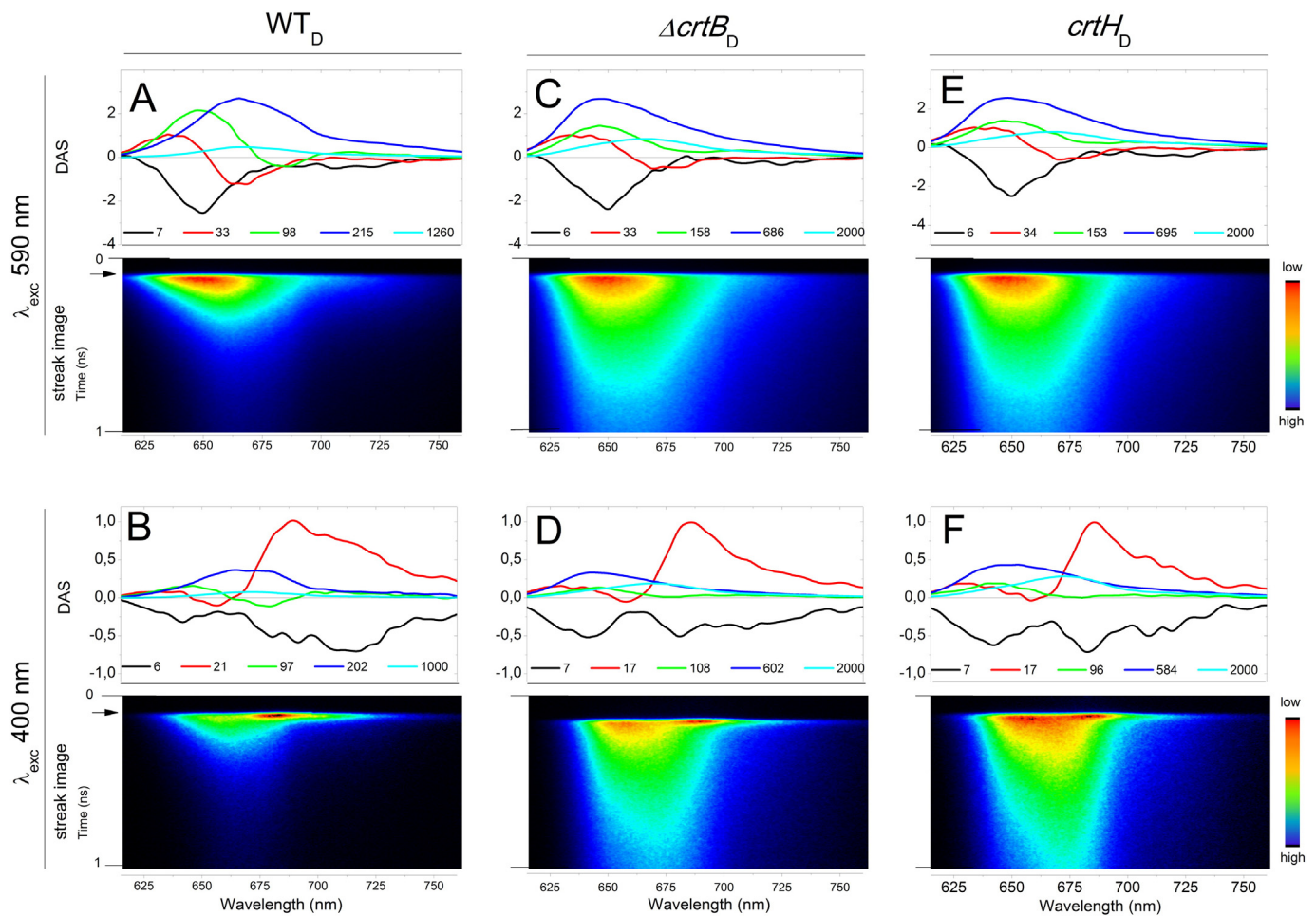


Fig. 5. Streak images and decay-associated spectra of dark grown strains. Data obtained for WT_D (A, B), $\Delta crtB$ _D (C, D) and $crtH$ _{LAHG} (E, F) cells are shown. DAS were obtained from global fitting of the time-resolved fluorescence data recorded with the streak-camera setup. The corresponding lifetimes are given in the figures in ps. The excitation wavelengths were 590 nm and 400 nm, as indicated. The spectra are normalized to the positive peak of the second (red color line) lifetime component. Streak images show 1 ns time windows of the fluorescence decays. Arrows represent the start of the fluorescence.

533 has spectral features that are very similar to those of $crtH_L$ cells and they
 534 are characteristic for PC rods. The three faster components all show
 535 down-hill EET characteristics somewhat similar to those of WT cells.
 536 However, there is no clear proof for EET to PSII, since no PSII decay component
 537 can be resolved from the data. The longest lifetime components
 538 probably represent the fluorescence emitted predominantly from the
 539 terminal emitter of the PBSs that do not transfer their energy to PSII.
 540 As was also observed for the other Car mutants (Fig. 4 and Supplemental
 541 Fig. 2), the red shoulder of the PSI fluorescence emission above 700 nm
 542 has decreased significantly for $\Delta crtB$ _D and $crtH$ _D cells upon 400 nm
 543 excitation.

544 3.5. Identification of phycobiliprotein fractions separated by sucrose 545 gradient

546 In order to determine to which extent PBSs assemble in the absence
 547 or under limited availability of Cars, PBSs were isolated from the different
 548 Car mutant strains and the assembled PBSs were purified using
 549 sucrose density gradient centrifugation. The PBS bands from $crtH_L$,
 550 $\Delta crtB$ _D and $crtH$ _D cells appeared to be shifted to lower densities suggesting
 551 reduced size, and two additional low-density subfractions appeared
 552 (Figs. 6 and 7). The two low-density subfractions show very similar PC-
 553 like fluorescence spectra with a maximum at around 650 nm, suggesting
 554 that the fluorescence is emitted by the same pigments (Fig. 6).
 555 These results indicate that PC rods in two different aggregation states

are responsible for the unconnected PC fluorescence signal in the 556
 $\Delta crtB$ _D, $crtH$ _D and $crtH_L$ cells *in vivo*. 557

In order to obtain structural information about the assembled PBSs 558
 of the $\Delta crtB$ and $crtH$ mutants, the protein composition of their PBSs 559
 was analyzed by denaturing Tricine-SDS gel electrophoresis (Fig. 6). 560
 Based on their molecular mass, the individual proteins can easily be 561
 identified [34,35]. The results show that the amount of rod linkers L_R^{30} 562
 and L_R^{33} is drastically reduced in PBSs from $\Delta crtB$ _D and $crtH_L$. The L_R^{30} 563
 and L_R^{33} rod linker proteins are necessary for connecting the PC units 564
 to each other [35]. The decreased amount of the linker proteins 565
 indicates that the PC rods of the mutant PBSs are reduced in size and 566
 contain predominantly one PC hexameric unit instead of three as is 567
 characteristic for WT [35]. 568

569 3.6. Streak-camera measurements of phycobilisomes

Using the streak camera, EET was studied in PBSs isolated from WT_D 570
 and $\Delta crtB$ _D cells (Fig. 7). PBSs isolated from WT_L and WT_D did not show 571
 significant difference (Supplemental Fig. 3). The calculated DAS of WT 572
 PBSs are similar to those presented by Tian et al. [51] with an extra fluo- 573
 rescence decay component, with ~250–300 ps lifetime in our case. A 574
 similar extra component (maximum ~660 nm) was observed previously 575
 [44] and was ascribed to some distorted PBSs. The other components 576
 are a 6 ps component, reflecting energy redistribution within PC rods, 577
 20 ps corresponding to EET from PC to APC₆₆₀ and 80 ps characterizing 578
 EET from APC₆₆₀ to APC₆₈₀. The ~1.6 ns component corresponds to the 579

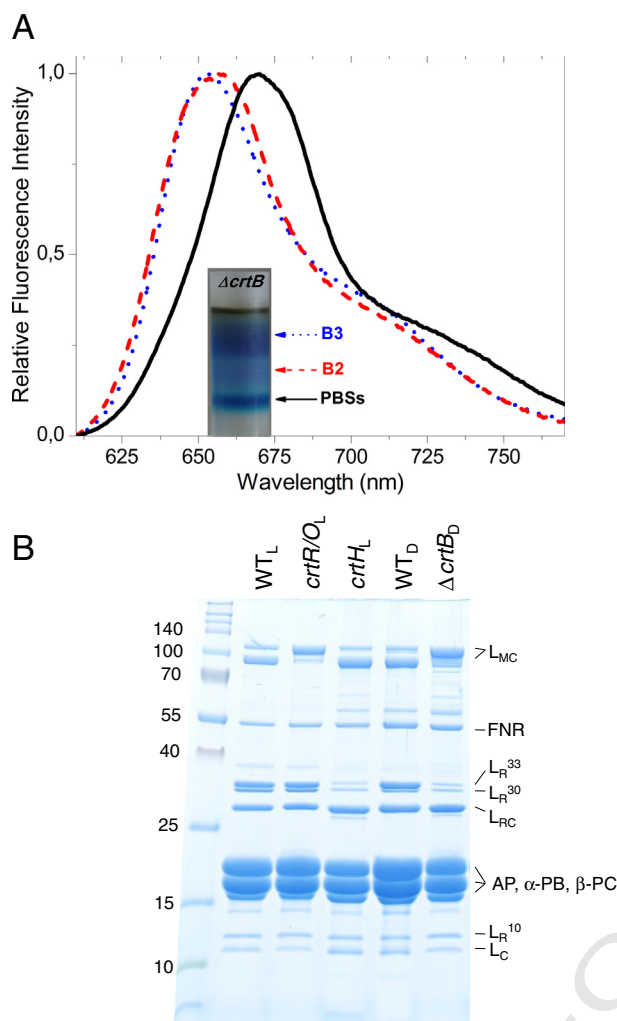


Fig. 6. Spectral properties and protein composition of the phycobilisomes and their subfractions. A, Sucrose density gradient profile and steady-state fluorescence spectra of the phycobiliprotein complexes from $\Delta crtB_D$ strain. B, Denaturing Tricine-SDS-PAGE of the isolated phycobilisomes of WT_L, crtR/O_L, crtH_L, WT_D and $\Delta crtB_D$ cells, respectively. The identities of the polypeptides are indicated on the right side, masses of the molecular marker are indicated in kDa on the left side.

580 excited-state lifetime of equilibrated PBSs. However, in $\Delta crtB$ PBSs
581 (Fig. 7) only 4 components can be resolved. The $\Delta crtB$ PBSs show re-
582 duced fluorescence in the PC region as compared to WT PBSs, and faster

EET from high- to low-energy pigments. This is ascribed to a shortening
583 of the PC rods, which is consistent with the results of the protein analy-
584 sis of isolated PBSs.
585

3.7. Fluorescence Lifetime Imaging Microscopy measurements

The crtH_L strain shows a WT-like thylakoid organization (Fig. 2) without any apparent indication of disconnected TEs of PBSs (Fig. 4), while a substantial number of unattached PC rods are present. Therefore, this mutant provides an excellent tool for studying the intracellular localization of the detached rod units. FLIM images of crtH_L cells were collected, using a 647/57 nm band pass filter (Fig. 8), which preferentially detects fluorescence of detached PC rods. Global analysis of the images allowed separation of three lifetimes, namely 66, 264 and 764 ps (Fig. 8). The average lifetimes are significantly longer in the center of the cells.

Although the fitted lifetimes for the FLIM images differ from those of the streak-camera measurements due to differences in time resolution and detection window, a clear correlation is present (for more FLIM images see Supplemental Fig. 1). The 66 ps component probably originates from EET in assembled PBSs. The 264 ps is a relatively short lifetime component, and therefore it is ascribed to photochemically quenched PBSs and/or PSII. The longer 764 ps component mainly represents detached PC rods; the corresponding spatial distribution is shown in Fig. 8 (panel D). This component has a relatively high contribution in the central region of the cells while it is clearly lower along the cell wall. In contrast, the two short components show opposite behavior, they have the highest contribution along the cell wall. The results show that the detached PC rod fractions (with 764 ps lifetime) are not co-localized with the thylakoid membranes in crtH_L cells, but are mainly present in the center of the cells.

4. Discussion

4.1. Carotenoids play a role in the formation of thylakoid membranes

The presence of Cars is known to be essential for preserving the integrity of thylakoid membranes [4,10], as indicated by the observation that Car-deficient mutants contain thylakoids with largely fragmented membrane sheets (Fig. 2) [4,10]. One might argue that the thylakoid fragmentation can be attributed to the decrease of PSII protein content due to the lack of Cars (Fig. 3), but this assumption can be ruled out based on the fact that a PSII-deficient mutant shows normal thylakoid sheets [52]. Severely fragmented thylakoids were observed in the absence of fucosylated myxoxanthophyll [4], suggesting a membrane-stabilizing function for this Car. In our experiments the xanthophyll-

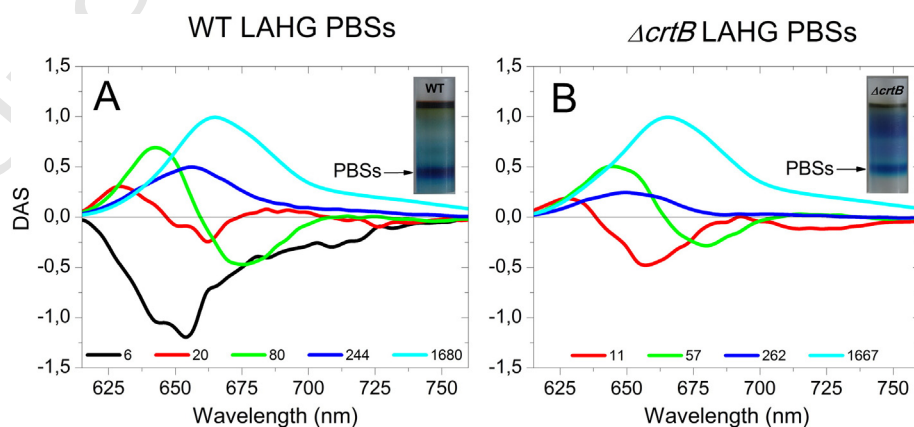
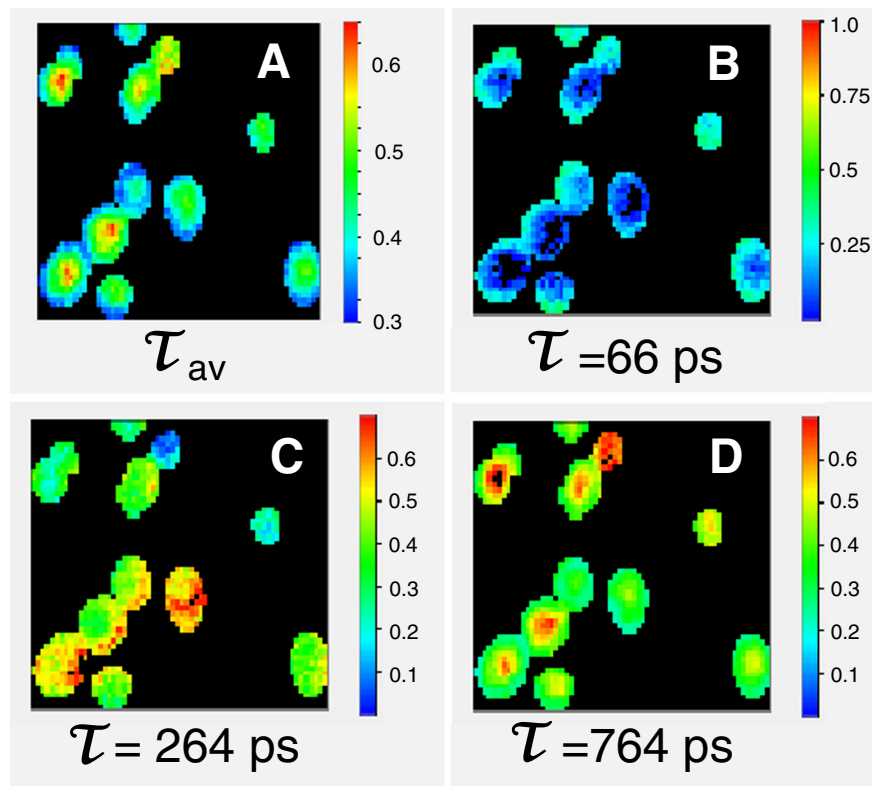


Fig. 7. Decay-associated spectra of isolated phycobilisomes. PBSs of WT_D (A) and $\Delta crtB_D$ (B) strains were studied by streak-camera setup using 590 nm excitation light. The corresponding lifetimes are given in the figures in ps. The spectra are normalized to the longest (cyan color line) lifetime component. The sucrose gradient profiles of the phycobilisomes are presented in the right upper corner.



Q3 Fig. 8. Fluorescence Lifetime Imaging Microscopy (FLIM) images of *crtH_L* cells. FLIM images were detected through a BP 647/58 bandpass filter. Images of calculated average lifetimes are given in ns (A). Distribution of the individual lifetime components as obtained from global analysis (B, C and D). Colors represent the relative contribution.

deficient (*crtR/O_L*) mutant possesses properly organized thylakoid membranes (Fig. 2 and [10]). In this mutant the deoxy-myxol-2'-di-methyl-fucoside intermediate of myxoxanthophyll biosynthesis, in addition to β -carotene [27,53] may replace myxoxanthophyll due to its similar chemical structure. It seems that the fucose molecule attached to the myxoxanthophyll has a major role in the formation of thylakoids, with a possible contribution of β -carotene as well.

4.2. β -Carotene is necessary for photosystem I trimerization

In cyanobacteria, especially when grown under low-light intensity, most PSI is found in trimeric form [54,55]. The crystal structure of PSI trimer from *T. elongatus* has revealed the presence of 22 β -carotene molecules per monomer [12,56]. In the present study we demonstrate that the Car-deficient $\Delta crtB$ mutant contains predominantly PSI monomers and only a few PSI trimers. (Figs. 3 and 4) [30]. Despite the relative abundance of Cars in PSI, the basic function of PSI is only slightly affected in a Car-deficient mutant [57], similar to what was observed for green algae [3]. However, the increased amount of monomers could be attributed to the destabilization of the PSI trimers, which disassemble during the sample preparation. The *in vivo* decrease of PSI trimers as compared to the monomers was confirmed using picosecond fluorescence measurements. Since PSI trimers in general contain more long-wavelength Chls (LWCs) than PSI monomers [58,59], the substantial decrease of the LWCs in the PSI fluorescence signal of Car-deficient cells (Fig. 5 and Supplemental Fig. 2) also indicates a considerable decrease in the trimer/monomer ratio as compared to WT cells. However, we cannot exclude that the decrease of the red Chl contribution is due to changes in the local environments of some of these Chls when carotenoids are not present. In the Car deficient cells PSI trimers appeared to be less resistant against SDS than PSI trimers from WT cells (Fig. 3) and in the mutant the interaction of the PsaL subunit with the PSI complex is weaker (Fig. 3). The PsaL protein is necessary for PSI trimer formation [56,60] and, according to the crystal structure of trimeric PSI, it is in

close contact with three β -carotenes [56,60]. These β -carotenes are not in the vicinity of any Chl *a* molecules and were hypothesized to be involved in trimer stabilization [12,55,56]. Similarly, the (light-grown) *crtH_L* cells, which have a limited availability of Cars, including β -carotene (Fig. 1) show an increased relative amount of monomeric PSI, whereas the binding of PsaL to monomeric PSI is weaker (Fig. 3). Probably the lack of the structurally important “linker” Cars leads to the destabilization of PsaL binding, and thus to a destabilization of the PSI trimer.

Previously, xanthophyll molecules have also been observed in PSI preparations [54,57,61]. This might be explained by co-purification of xanthophylls, or by assuming that PSI trimers contain loosely connected xanthophylls, which are lost upon crystallization. Klodawska et al. observed a significant increase in the amount of echinenone in PSI trimer samples as compared to the monomer samples and hypothesized a possible role of echinenone in trimer formation [54]. Remarkably, in xanthophyll-deficient (*crtR/O_L*) cells protein analysis also showed slightly less PSI trimers and relatively more PSI monomers than in WT cells (Fig. 3), which is accompanied by a decrease of LWC contribution to the fluorescence (Fig. 4 and Supplemental Fig. 2). Unlike in Car-less cells, in xanthophyll deficient cells the PsaL protein binds to the PSI monomer with similar affinity as in WT_L or WT_D cells, and thus it is also present in the monomeric PSI complex (Fig. 3). It is noteworthy that in cyanobacteria the lack of xanthophylls does not induce a decrease of the PSI protein level in thylakoid membranes as compared to PSII as was observed in higher plants [62]. In plants xanthophyll deficiency induced the almost complete lack of the PSI complex due to the suppressed translation and accelerated degradation of PsaA and PsaB subunits [63].

The different affinity of the PsaL protein to the PSI complex in Car-deficient ($\Delta crtB$) and xanthophyll-deficient (*crtR/O*) cells implies that the increase in PSI monomers may have different reasons in the two mutants. We propose that, in addition to PsaL [56,60] and a phosphatidylglycerol molecule [64], β -carotenes are also necessary for

the stabilization of the trimerization domain, most probably *via* stabilizing the interaction between PSI and the PsaL protein, while xanthophylls might surround the PSI trimer and externally stabilize it.

4.3. Influence of carotenoids on photosystem II structure

Although PSII contains less Cars than PSI (12 vs. 22 β -carotenes per monomer, in *T. elongatus*) [13,65], Cars are essential for the assembly of PSII dimers in cyanobacteria [30,66] and green algae as well [3]. Accordingly, in Car-less *Synechocystis* cells only trace amounts of the partially assembled (CP43-depleted) RC47:PSII subcomplex can be detected (Fig. 3), as was demonstrated earlier [30]. We also could not distinguish a clear PSII fluorescence signal from the Car-deficient cells (Fig. 5) [29]. Our results show that the production of carotenoids by photoisomerization only, without the CrhH-catalyzed pathway, results in partially impaired PSII functioning (*crtH_L*, Fig. 4) similar to what was found in rice when the homologue enzyme of CrhH was knocked out [67]. The relatively fast fluorescence decay observed in these cells (Fig. 4), as compared to Δ *crtB* cells, indicates a considerable amount of functional PSII, which is capable of photochemical quenching. However, the amount of active PSII complexes seems to be lower than in WT cells, unlike what was proposed by Masamoto et al. [29].

Our protein analyses obtained for xanthophyll deficient mutants revealed a significant decrease in the amount of detected PSII dimers (Fig. 3) in low-light grown cells, but no corresponding change was seen in the PSII related *in vivo* fluorescence (Fig. 4 blue color line DAS upon 400 nm excitation), indicating that PSII is probably less stable and disassembles in the PAGE. These observations support the notion that the assembly of functional PSII requires the presence of β -carotene, whereas xanthophylls seem to have a minor, stabilizing function even under low-light conditions.

4.4. Proper assembly of phycobilisomes requires β -carotene

Although there is no report on the presence of Cars in PBSs, we have found that they strongly influence PBS integrity. In Car-deficient (Δ *crtB*) cells time-resolved fluorescence at room temperature revealed a high level of energetically disconnected, non-transferring PC units, which are not present in WT cells (Fig. 5). Further measurements on this Car-less mutant showed the presence of assembled PBSs as well, but with reduced size. In the mutant PBSs we detected faster excited-state equilibration with the cores using time-resolved fluorescence (Fig. 8) which is attributed to the reduced length of radial rods, a notion confirmed by their protein composition (Fig. 6). Our results imply that Car-deficient PBSs contain predominantly rods with only one or two hexameric PC units, although small amounts of full-length rods, composed of three hexameric units, are also present.

Besides the fully assembled PBSs, two fractions of phycobiliprotein complexes were separated by sucrose density gradient in the Car-less mutant (Fig. 6). Both fractions show the typical PC fluorescence (Fig. 6), but they differ in size. We conclude that in Car-deficient cells most of the PBSs possess a reduced number of the peripheral PC rods, and that part of the PC is present as unconnected units. It should be noted that the xanthophyll-less *crtR/O* mutant contains properly assembled PBSs, similar to WT cells (Fig. 7). Therefore, we conclude that the lack of β -carotene or fusosulated myxoxanthophyll may cause PBS distortion. Assuming a direct PBS-stabilizing role for Cars would imply the presence of a Car molecule inside or in the vicinity of the PBS rods, but up to now there is no evidence supporting this assumption. Therefore, at present an indirect effect of the Car composition on the structure of the PBSs seems more likely.

The decreased level of the rod linker proteins in the carotenoid deficient mutant would explain the abundance of unconnected PC units. The absence of the last two peripheral rod units observed in PBSs of Car-deficient cells also occurs in the mutant lacking L_R^{33} , the 33 kDa rod linker, which connects the last two hexamers to the basal PC rod

unit [35]. Surprisingly, the L_R^{33} -deficient mutant exhibits only one fraction of the detached rods [35], while two are present in the Car-less mutant. This difference suggests distinct reasons for improperly assembled PBSs in the two mutants. In light-grown *crtH* cells the Car content is almost restored to the WT level (Fig. 1) [28]. Our results show that the Car synthesis in *crtH_L* cells is insufficient to warrant assembly and stability of pigment-protein complexes to the same level as for WT cells (Figs. 3 and 4), which is most apparent in case of the PBSs. In this mutant, independent of the presence of light, the PBSs are distorted to a similar extent as for the carotenoid deficient (Δ *crtB*) cells (Figs. 4 and 5). We can speculate that under limited carotenoid availability β -carotene incorporates preferentially into those proteins that are involved in the most essential processes; e.g. in the light-grown *crtH* cells the major part of photosynthetic reaction centers seems to be functional while the PBSs are largely unassembled.

The light-grown *crtH* strain shows a WT-like thylakoid organization (Fig. 2) but a detached population of PC rods is present while the APC cores of the PBSs are still transferring energy to the PSs (Fig. 4). We used this mutant for studying the intracellular localization of the detached rod units. FLIM experiments demonstrate that the fluorescence decay component originating from PC (Fig. 4) has a higher relative contribution in the middle of the cells (Fig. 9). Therefore, we can conclude that the detached rod units are accumulated in the cytoplasm, away from the thylakoid membrane. A similar dislocation of disconnected rod units was observed by Tamary et al. [68] upon exposing the cells to extreme-high intensity illumination.

The lack of PSII itself cannot be the reason for the improper assembly of PBSs in the absence of Cars, since PBSs are fully compiled in WT cells even under dark condition, when a considerable amount of PBSs is unattached and photochemically unquenched (Figs. 5 and 8), or in a mutant containing only a trace amounts of Chl [69]. Furthermore, in *crtH_L* cells a high amount of unconnected PC units was detected, although a significant amount of PSII complexes was observed (Fig. 3).

Based on our results, we have to conclude that proper PBS assembly requires the presence of β -carotene in the cells.

4.5. Concluding remarks

Although it is generally believed that xanthophylls do not play an important role in cyanobacterial photosynthesis under low-light conditions, our current results demonstrate that this picture has to be modified. Indeed the excitation energy transfer within the PBSs and the PSs, as well as the charge separation within PSI and PSII seem to be unaffected in the absence of xanthophylls. However, it remains unclear how xanthophylls stabilize the PSI trimers and PSII dimers, because their presence in PSI and PSII has hitherto not been observed.

The study of the *crtH_L* cells shows that in case of limited carotenoid formation, the oligomerization of PSI and PSII is substantially disturbed, although PSI and PSII are still assembled and the thylakoid membrane is similarly organized. EET from PBSs to PSs is largely absent, which is not only due to a decrease in PSI and PSII oligomerization but also to the fact that many PBSs are not fully assembled. Results show that a large part of the PC rods do not attach to the PBS core and these non-attached PC complexes are not located in the vicinity of the thylakoid membranes. It seems that only fully assembled PBSs attach to the PSs. Δ *crtB_D* and *crtH_D* cells do not have any or hardly any carotenoids and the thylakoid structure appears to be completely disturbed. PSII is not formed, whereas PSI is formed but less stable and occurs mainly in its monomeric form. Again, a large part of the PC rods is not attached to the PBS core, which is accompanied by a drastic reduction of linker proteins in the mutant PBSs. This reduction is surprising because carotenoids have never been found as part of the PBSs. One might thus speculate that xanthophylls and carotenoids are essential ingredients of the assembly and maintenance machinery of the photosynthetic complexes in the cells.

Acknowledgments

The authors thank Arie van Hoek for technical help with the time-resolved measurements, and Prof. Árpád Párducz for providing the electron micrographs in Fig. 2. Special thanks go to Anna Sallai Kunné for the phycobilisome preparation, Roberta Croce, Miklós Szekeres and Bettina Ughy for critical reading of the manuscript.

This work was supported by the Sandwich PhD program of Wageningen University (to T.T.), by the HARVEST Marie Curie Research Training Network (PITN-GA-2009-238017) (to V.C.), grant OTKA K108411 and K112688 from the Hungarian Scientific Research Fund (to T.T. and GG, respectively), Social Renewal Operational Programs (TAMOP-4.2.2/B-10/1-2010-0012 to T.T., TAMOP-4.2.2.A-11/1/KONV-2012-0047 to L.K.), A*STAR Singapore (NIH-A*STAR TET_10-1-2011-0279, to G.G.), P501/12/G055 of the Grant Agency of the Czech republic (to J. Knoppová and J. K.) and bilateral project of Academy of Science of the Czech Republic and Hungary (HU/2013/06 to Z.G. and J.K.).

Appendix A. Supplementary data

Supplementary data to this article can be found online at <http://dx.doi.org/10.1016/j.bbabi.2015.05.020>.

References

[1] C.I. Cazzonelli, Carotenoids in nature: insights from plants and beyond, *Funct. Plant Biol.* 38 (2011) 833–847.

[2] O. Sozer, M. Kis, Z. Gombos, B. Ughy, Proteins, glycerolipids and carotenoids in the functional photosystem II architecture, *Front. Biosci. (Landmark Ed.)* 16 (2011) 619–643.

[3] S. Santabarbara, A.P. Casazza, K. Ali, C.K. Economou, T. Wannathong, F. Zito, K.E. Redding, F. Rappaport, S. Purton, The requirement for carotenoids in the assembly and function of the photosynthetic complexes in *Chlamydomonas reinhardtii*, *Plant Physiol.* 161 (2013) 535–546.

[4] H.E. Mohamed, A.M.L. van de Meene, R.W. Roberson, W.F.J. Vermaas, Myxoxanthophyll is required for normal cell wall structure and thylakoid organization in the cyanobacterium, *Synechocystis* sp strain PCC 6803, *J. Bacteriol.* 187 (2005) 6883–6892.

[5] W.I. Gruszecki, K. Strzalka, Carotenoids as modulators of lipid membrane physical properties, *Biochim. Biophys. Acta* 1740 (2005) 108–115.

[6] R. Croce, H. van Amerongen, Natural strategies for photosynthetic light harvesting, *Nat. Chem. Biol.* 10 (2014) 492–501.

[7] K. Stamatakis, M. Tsimilli-Michael, G.C. Papageorgiou, On the question of the light-harvesting role of beta-carotene in photosystem II and photosystem I core complexes, *Plant Physiol. Biochem.* (2014).

[8] L. Schafer, M. Sandmann, S. Woitsch, G. Sandmann, Coordinate up-regulation of carotenoid biosynthesis as a response to light stress in *Synechococcus* PCC 7942, *Plant Cell Environ.* 29 (2006) 1349–1356.

[9] S. Cazzaniga, Z. Li, K.K. Niyogi, R. Bassi, L. Dall'Osto, The *Arabidopsis* szl1 mutant reveals a critical role of beta-carotene in photosystem I photoprotection, *Plant Physiol.* 159 (2012) 1745–1758.

[10] I. Domonkos, M. Kis, Z. Gombos, B. Ughy, Carotenoids, versatile components of oxygenic photosynthesis, *Prog. Lipid Res.* 52 (2013) 539–561.

[11] S. Takaichi, M. Mochimaru, Carotenoids and carotenogenesis in cyanobacteria: unique ketocarotenoids and carotenoid glycosides, *Cell. Mol. Life Sci.* 64 (2007) 2607–2619.

[12] P. Jordan, P. Fromme, H.T. Witt, O. Klukas, W. Saenger, N. Krauss, Three-dimensional structure of cyanobacterial photosystem I at 2.5 Å resolution, *Nature* 411 (2001) 909–917.

[13] A. Guskov, J. Kern, A. Gabdulkhakov, M. Broser, A. Zouni, W. Saenger, Cyanobacterial photosystem II at 2.9-Å resolution and the role of quinones, lipids, channels and chloride, *Nat. Struct. Mol. Biol.* 16 (2009) 334–342.

[14] G. Kurisu, H.M. Zhang, J.L. Smith, W.A. Cramer, Structure of the cytochrome b(6)f complex of oxygenic photosynthesis: tuning the cavity, *Science* 302 (2003) 1009–1014.

[15] J. Knoppová, R. Sobotka, M. Tichý, J. Yu, P. Konik, P. Halada, P.J. Nixon, J. Komenda, Discovery of a chlorophyll binding protein complex involved in the early steps of photosystem II assembly in *Synechocystis*, *Plant Cell* 26 (2014) 1200–1212.

[16] D. Kirilovsky, C.A. Kerfeld, The orange carotenoid protein: a blue-green light photoactive protein, *Photochem. Photobiol. Sci.* 12 (2013) 1135–1143.

[17] L. Tian, I.H. van Stokkum, R.B. Koehorst, A. Jongerijs, D. Kirilovsky, H. van Amerongen, Site, rate, and mechanism of photoprotective quenching in cyanobacteria, *J. Am. Chem. Soc.* 133 (2011) 18304–18311.

[18] A. Sedoud, R. Lopez-Igual, A.U. Rehman, A. Wilson, F. Perreau, C. Boulay, I. Vass, A. Krieger-Liszky, D. Kirilovsky, The cyanobacterial photoactive orange carotenoid protein is an excellent singlet oxygen quencher, *Plant Cell* 26 (2014) 1781–1791.

[19] C. Punginelli, A. Wilson, J.M. Routaboul, D. Kirilovsky, Influence of zeaxanthin and echinenone binding on the activity of the orange carotenoid protein, *Biochim. Biophys. Acta* 1787 (2009) 280–288.

[20] S. Steiger, L. Schafer, G. Sandmann, High-light-dependent upregulation of carotenoids and their antioxidative properties in the cyanobacterium *Synechocystis* PCC 6803, *J. Photochem. Photobiol. B Biol.* 52 (1999) 14–18.

[21] I. Domonkos, P. Malec, H. Laczko-Dobos, O. Sozer, K. Klodawska, H. Wada, K. Strzalka, Z. Gombos, Phosphatidylglycerol depletion induces an increase in myxoxanthophyll biosynthetic activity in *Synechocystis* PCC 6803 cells, *Plant Cell Physiol.* 50 (2009) 374–382.

[22] K. Masamoto, O. Zsiros, Z. Gombos, Accumulation of zeaxanthin in cytoplasmic membranes of the cyanobacterium *Synechococcus* sp. strain PCC 7942 grown under high light condition, *J. Plant Physiol.* 155 (1999) 136–138.

[23] Y. Kusama, S. Inoue, H. Jimbo, S. Takaichi, K. Sonoike, Y. Hihara, Y. Nishiyama, Zeaxanthin and echinenone protect the repair of photosystem II from inhibition by singlet oxygen in *Synechocystis* sp. PCC 6803, *Plant Cell Physiol.* (2015).

[24] J.E. Graham, D.A. Bryant, The biosynthetic pathway for synechoxanthin, an aromatic carotenoid synthesized by the euryhaline, unicellular cyanobacterium *Synechococcus* sp. strain PCC 7002, *J. Bacteriol.* 190 (2008) 7966–7974.

[25] Y. Zhu, J.E. Graham, M. Ludwig, W. Xiong, R.M. Alvey, G. Shen, D.A. Bryant, Roles of xanthophyll carotenoids in protection against photoinhibition and oxidative stress in the cyanobacterium *Synechococcus* sp strain PCC 7002, *Arch. Biochem. Biophys.* 504 (2010) 86–99.

[26] L. Schafer, A. Vioque, G. Sandmann, Functional in situ evaluation of photo synthesis-protecting carotenoids in mutants of the cyanobacterium *Synechocystis* PCC 6803, *J. Photochem. Photobiol. B Biol.* 78 (2005) 195–201.

[27] D. Lagarde, W. Vermaas, The zeaxanthin biosynthesis enzyme beta-carotene hydroxylase is involved in myxoxanthophyll synthesis in *Synechocystis* sp. PCC 6803, *FEBS Lett.* 454 (1999) 247–251.

[28] K. Masamoto, H. Wada, T. Kaneko, S. Takaichi, Identification of a gene required for cis-to-trans carotene isomerization in carotenogenesis of the cyanobacterium *Synechocystis* sp PCC 6803, *Plant Cell Physiol.* 42 (2001) 1398–1402.

[29] K. Masamoto, S. Hisatomi, I. Sakurai, Z. Gombos, H. Wada, Requirement of carotene isomerization for the assembly of photosystem II in *Synechocystis* sp PCC 6803, *Plant Cell Physiol.* 45 (2004) 1325–1329.

[30] O. Sozer, J. Komenda, B. Ughy, I. Domonkos, H. Laczko-Dobos, P. Malec, Z. Gombos, M. Kis, Involvement of carotenoids in the synthesis and assembly of protein subunits of photosynthetic reaction centers of *Synechocystis* sp PCC 6803, *Plant Cell Physiol.* 51 (2010) 823–835.

[31] S.L. Anderson, L. McIntosh, Light-activated heterotrophic growth of the cyanobacterium *Synechocystis* sp strain PCC 6803 – a blue-light-requiring process, *J. Bacteriol.* 173 (1991) 2761–2767.

[32] N.V. Karapetyan, Y.V. Bolychevtseva, N.P. Yurina, I.V. Terekhova, V.V. Shubin, M. Brecht, Long-wavelength chlorophylls in photosystem I of cyanobacteria: origin, localization, and functions, 79 (2014) 213–220.

[33] C.W. Mullineaux, Excitation-energy transfer from phycobilisomes to photosystem I in a cyanobacterial mutant lacking photosystem II, *Biochim. Biophys. Acta* 1184 (1994) 71–77.

[34] A.A. Arteni, G. Ajlani, E.J. Boekema, Structural organisation of phycobilisomes from *Synechocystis* sp strain PCC6803 and their interaction with the membrane, *Biochim. Biophys. Acta* 1787 (2009) 272–279.

[35] B. Ughy, G. Ajlani, Phycobilisome rod mutants in *Synechocystis* sp strain PCC6803, *Microbiology* 150 (2004) 4147–4156.

[36] D. Jallet, M. Gwizdala, D. Kirilovsky, ApcD, ApcF and ApcE are not required for the orange carotenoid protein related phycobilisome fluorescence quenching in the cyanobacterium *Synechocystis* PCC 6803, *Biochim. Biophys. Acta* 1817 (2012) 1418–1427.

[37] M.K. Ashby, C.W. Mullineaux, The role of ApcD and ApcF in energy transfer from phycobilisomes to PSI and PSII in a cyanobacterium, *Photosynth. Res.* 61 (1999) 169–179.

[38] M.M. Allen, Simple conditions for growth of unicellular blue-green algae on plates, *J. Phycol.* 4 (1968) 1–4.

[39] R.F.C. Mantoura, C.A. Llewellyn, The rapid-determination of algal chlorophyll and carotenoid-pigments and their breakdown products in natural-waters by reverse-phase high-performance liquid-chromatography, *Anal. Chim. Acta* 151 (1983) 297–314.

[40] H. Laczko-Dobos, B. Ughy, S.Z. Toth, J. Komenda, O. Zsiros, I. Domonkos, A. Párducz, B. Bogos, M. Komura, S. Itoh, Z. Gombos, Role of phosphatidylglycerol in the function and assembly of photosystem II reaction center, studied in a *cdsA*-inactivated PAL mutant strain of *Synechocystis* sp. PCC6803 that lacks phycobilisomes, *Biochim. Biophys. Acta* 1777 (2008) 1184–1194.

[41] F. Garnier, J.P. Dubacq, J.C. Thomas, Evidence for a transient association of new proteins with the *Spirulina maxima* phycobilisome in relation to light intensity, *Plant Physiol.* 106 (1994) 747–754.

[42] J. Komenda, V. Reisinger, B.C. Muller, M. Dobakova, B. Granvogel, L.A. Eichacker, Accumulation of the D2 protein is a key regulatory step for assembly of the photosystem II reaction center complex in *Synechocystis* PCC 6803, *J. Biol. Chem.* 279 (2004) 48620–48629.

[43] H. Schagger, Tricine-SDS-PAGE, *Nat. Protoc.* 1 (2006) 16–22.

[44] S. Krumova, S. Laptanok, J. Borst, B. Ughy, Z. Gombos, G. Ajlani, H. van Amerongen, Monitoring photosynthesis in individual cells of *Synechocystis* sp. PCC 6803 on a picosecond timescale, *Biophys. J.* 99 (2010) 2006–2015.

[45] S.P. Laptanok, J.J. Snellenburg, C.A. Bucherl, K.R. Konrad, J.W. Borst, Global analysis of FRET-FILM data in live plant cells, *Methods Mol. Biol.* 1076 (2014) 481–502.

[46] S.P. Laptanok, J.W. Borst, K.M. Mullen, I.H.M. van Stokkum, A.J.W.G. Visser, H. van Amerongen, Global analysis of Förster resonance energy transfer in live cells 972

- 973 measured by fluorescence lifetime imaging microscopy exploiting the rise time of
974 acceptor fluorescence, *Phys. Chem. Chem. Phys.* 12 (2010) 7593–7602.
- 975 [47] B. Van Oort, S. Murali, E. Wientjes, R.B.M. Koehorst, R.B. Spruijt, A. van Hoek, R.
976 Croce, H. van Amerongen, Ultrafast resonance energy transfer from a site-
977 specifically attached fluorescent chromophore reveals the folding of the N-
978 terminal domain of CP29, *Chem. Phys.* 357 (2009) 113–119.
- 979 [48] K.M. Mullen, I.H.M. van Stokkum, TIMP: an R package for modeling multi-way spec-
980 troscopic measurements, *J. Stat. Softw.* 18 (2007).
- 981 [49] M. Liberton, L.E. Page, W.B. O'Dell, H. O'Neill, E. Mamontov, V.S. Urban, H.B. Pakrasi,
982 Organization and flexibility of cyanobacterial thylakoid membranes examined by
983 neutron scattering, *J. Biol. Chem.* 288 (2013) 3632–3640.
- 984 [50] K. Broess, G. Trinkunas, A. van Hoek, R. Croce, H. van Amerongen, Determination of
985 the excitation migration time in photosystem II consequences for the membrane or-
986 ganization and charge separation parameters, *Biochim. Biophys. Acta* 1777 (2008)
987 404–409.
- 988 [51] L. Tian, M. Gwizdala, I.H. van Stokkum, R.B. Koehorst, D. Kirilovsky, H. van
989 Amerongen, Picosecond kinetics of light harvesting and photoprotective quenching
990 in wild-type and mutant phycobilisomes isolated from the cyanobacterium
991 *Synechocystis* PCC 6803, *Biophys. J.* 102 (2012) 1692–1700.
- 992 [52] F. Nilsson, D.J. Simpson, C. Jansson, B. Andersson, Ultrastructural and biochemical
993 characterization of a *Synechocystis* 6803 mutant with inactivated Psba genes, *Arch.*
994 *Biochem. Biophys.* 295 (1992) 340–347.
- 995 [53] S. Takaichi, T. Maoka, K. Masamoto, Myxoxanthophyll in *Synechocystis* sp. PCC 6803
996 is myxol 2'-dimethyl-fucoside, (3R,2'S)-myxol 2'-(2,4-di-O-methyl-alpha-L-
997 fucoside), not rhamnoside, *Plant Cell Physiol.* 42 (2001) 756–762.
- 998 [54] K. Klodawska, L. Kovacs, Z. Varkonyi, M. Kis, O. Sozer, H. Laczko-Dobos, O. Kobori, I.
999 Domonkos, K. Strzalka, Z. Gombos, P. Malec, Elevated growth temperature can en-
1000 hance photosystem I trimer formation and affects xanthophyll biosynthesis in cy-
1001 anobacterium *Synechocystis* sp. PCC6803 cells, *Plant Cell Physiol.* 56 (2014) 558–571.
- 1002 [55] I. Grotjohann, P. Fromme, Structure of cyanobacterial photosystem I, *Photosynth.*
1003 *Res.* 85 (2005) 51–72.
- 1004 [56] P. Fromme, P. Jordan, N. Krauss, Structure of photosystem I, *Biochim. Biophys. Acta*
1005 1507 (2001) 5–31.
- 1006 [57] J.A. Bautista, F. Rappaport, M. Guergova-Kuras, R.O. Cohen, J.H. Golbeck, J.Y. Wang, D.
1007 Beal, B.A. Diner, Biochemical and biophysical characterization of photosystem I from
1008 phytoene desaturase and ζ -carotene desaturase deletion mutants of *Synechocystis*
1009 sp PCC 6803, *J. Biol. Chem.* 280 (2005) 20030–20041.
- 1010 [58] B. Gobets, R. van Grondelle, Energy transfer and trapping in photosystem I, *Biochim.*
1011 *Biophys. Acta* 1507 (2001) 80–99.
- 1012 [59] E. El-Mohsawy, M.J. Kopczak, E. Schlodder, M. Nowaczyk, H.E. Meyer, B. Warscheid,
1013 N.V. Karapetyan, M. Rögner, Structure and function of intact photosystem I mono-
1014 mers from the cyanobacterium *Thermosynechococcus elongatus*, *Biochemistry* 49
1015 (2010) 4740–4751.
- 1016 [60] V.P. Chitnis, P.R. Chitnis, PsaL subunit is required for the formation of photosystem I
1017 trimers in the cyanobacterium *Synechocystis* sp PCC 6803, *FEBS Lett.* 336 (1993)
1018 330–334.
- 1019 [61] J. Coufal, J. Hladik, D. Sofrova, The carotenoid content of photosystem I pigment-
1020 protein complexes of the cyanobacterium *Synechococcus elongatus*, *Photosynthetica*
1021 23 (1989) 603–616.
- 1022 [62] A. Fiore, L. Dall'Osto, S. Cazzaniga, G. Diretto, G. Giuliano, R. Bassi, A quadruple mu-
1023 tant of *Arabidopsis* reveals a beta-carotene hydroxylation activity for LUT1/CYP97C1
1024 and a regulatory role of xanthophylls on determination of the PSI/PSII ratio, *BMC*
1025 *Plant Biol.* 12 (2012) 50.
- 1026 [63] L. Dall'Osto, M. Piques, M. Ronzani, B. Molesini, A. Alboresi, S. Cazzaniga, R. Bassi, The
1027 *Arabidopsis* nox mutant lacking carotene hydroxylase activity reveals a critical role
1028 for xanthophylls in photosystem I biogenesis, *Plant Cell* 25 (2013) 591–608.
- 1029 [64] I. Domonkos, P. Malec, A. Sallai, L. Kovacs, K. Itoh, G.Z. Shen, B. Ughy, B. Bogos, I.
1030 Sakurai, M. Kis, K. Strzalka, H. Wada, S. Itoh, T. Farkas, Z. Gombos,
1031 Phosphatidylglycerol is essential for oligomerization of photosystem I reaction cen-
1032 ter, *Plant Physiol.* 134 (2004) 1471–1478.
- 1033 [65] B. Loll, J. Kern, W. Saenger, A. Zouni, J. Biesiadka, Towards complete cofactor ar-
1034 rangement in the 3.0 Angstrom resolution structure of photosystem II, *Nature* 438
1035 (2005) 1040–1044.
- 1036 [66] J.A. Bautista, C.A. Tracewell, E. Schlodder, F.X. Cunningham, G.W. Brudvig, B.A. Diner,
1037 Construction and characterization of genetically modified *Synechocystis* sp. PCC
1038 6803 photosystem II core complexes containing carotenoids with shorter π -
1039 conjugation than beta-carotene, *J. Biol. Chem.* 280 (2005) 38839–38850.
- 1040 [67] J.L. Wei, M. Xu, D.B. Zhang, H.L. Mi, The role of carotenoid isomerase in maintenance
1041 of photosynthetic oxygen evolution in rice plant, *Acta Biochim. Biophys. Sin.* 42
1042 (2010) 457–463.
- 1043 [68] E. Tamary, V. Kiss, R. Nevo, Z. Adam, G. Bernat, S. Rexroth, M. Roegner, Z. Reich,
1044 Structural and functional alterations of cyanobacterial phycobilisomes induced by
1045 high-light stress, *Biochim. Biophys. Acta* 1817 (2012) 319–327.
- 1046 [69] X.G. Liu, J.J. Zhao, Q.Y. Wu, Oxidative stress and metal ions effects on the cores of
1047 phycobilisomes in *Synechocystis* sp PCC 6803, *FEBS Lett.* 579 (2005) 4571–4576.